

# Study on the tribological properties between the aluminum alloy 7050-T7451 and the YG8 cemented carbide

Guiyu Li · Jianfeng Li · Jie Sun · Feng Jiang

Received: 3 May 2010 / Accepted: 26 July 2010 / Published online: 12 August 2010  
© Springer Science+Business Media, LLC 2010

**Abstract** The ball–disc friction experiments are performed by applying the YG8 cemented carbide ball and the aluminum alloy 7050-T7451 plate under high speed and high load, and then the wear depth of the groove was observed using white light interferometer. The average contact normal stress was calculated by the depth of the groove. The relationship between friction coefficient and average contact normal stress as well as sliding velocity is fitted with Minitab. It shows the friction coefficient decreases with the increasing of the sliding velocity and the average contact stress. The results provide certain theoretical basis to build the friction model and finite element model of machining Al alloy.

## Introduction

Aluminum alloys 7050-T7451 is a alloy of Al–Zn–Mg–Zr, which has high structural strength, higher fracture toughness, and good resistance to stress corrosion cracking, so that it is widely adopted in aeronautical manufacturing [1]. But the machinability of the aluminum alloys 7050-T7451 is not good because the tool is stucked easily and build-up-edge will appear. So the tribological properties between tool and work piece during machining is always the focus of cutting mechanism research [2]. In some of the most celebrated studies of high-speed friction, Bowden [3, 4] spun a steel ball to a very high rotational speed and then grabbed it

with other frictional samples or dropped it on another to achieve slip speeds as high as 800 m/s. Ogawa [5] in 1997 used a new testing technique, which provides the normal and the tangential impact force independently to understand the dynamic response of two bodies in contact. Rajagopalan [6] investigated the high strain rate behavior of engineering materials at normal pressures up to 100 MPa, slip speed up to 10 m/s and slip distances of approximately 10 mm. Most recently, plate-impact pressure-shear friction experiments were conducted by Irfan and Prakash [7] to understand time-resolved frictional characteristics during high-speed sliding of metal on metal. In a later study, by employing tribo-pairs comprising hard tool-steel against relatively low melt-point metals such as 7075-T6 Al alloy, Okada and Liou [8–10] investigated time-resolved growth of molten metal films during dry metal-on-metal slip under extreme interfacial conditions (normal stress ranging from 1 to 3 GPa and interfacial slip speeds in the range of 1–100 m/s). Fuping Yuan [11] achieved interfacial normal stress of up to 5 Gpa and slip speeds of approximately 250 m/s by employing a tribo-pair comprising of a hard tool-steel against a relatively low melt-point metal (7075-T6 Al alloy). The study on the tribological characteristics of engineering material trends to new testing method and high interfacial stress and high slip speed.

During aluminum alloy machining, the tribological characteristics between cutting tool and work piece play an important role in the cutting force, cutting temperature and surface quality of work piece. Therefore, the study of tribological properties is necessary to analyze the machinability of aluminum alloy. In the present article, the friction and wear behaviors between the cemented carbide ball and Al7050-T7451 disc under different rotational speed and different load were studied, which provide basic theory to reveal the tribological characteristics of Al7050-T7451.

G. Li (✉) · J. Li · J. Sun · F. Jiang  
School of Mechanical Engineering, ShanDong University,  
Jinan 250061, China  
e-mail: guiyukelly@gmail.com

G. Li · J. Li · J. Sun · F. Jiang  
Key Laboratory of High Efficiency and Clean Mechanical  
Manufacture, Shandong University, Jinan 250061, China

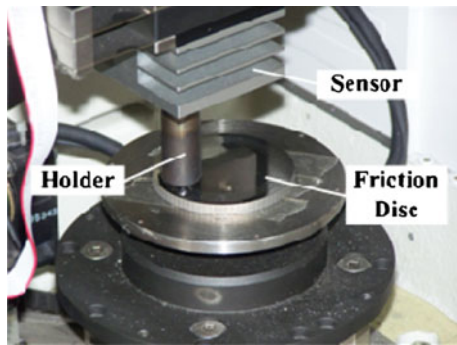


**Fig. 1** UMT-2 high temperature tribometer

### Details of ball-disc friction experiment

#### Equipment and specimens

The experimental tests were performed at room temperature in ambient air using UMT-2 high temperature tribometer as shown in Fig. 1. In this machine, the carriage is used to apply load through holder to the sliding contact specimens. The plate is allocated to rotate at a prescribed speed during the test process with the disc specimen stuck on.

According to the requirement to aluminum alloy 7050 of American Aluminum Industry Association (AA), the composition of testing material is listed in Table 1. The alloy is machined into a disc specimen with diameter of 60 mm and thickness of 8 mm, which is stuck on the plate and rotates with it. So the end surface of specimen should be smooth.

#### Procedures and parameters of test

The material of sliding ball was cemented carbide which is usually used as manufacturing milling cutter in aluminum alloy cutting. Before each test, the specimen surface was polished with flannelette and was cleaned with alcohol, so that the surface roughness could reach  $R_a = 0.2 \mu\text{m}$  to obtain a good contact between the disc specimen and sliding ball.

In the test, the sliding speeds  $v$  were set to 90, 120, 150, 180 m/min. Meanwhile, the normal loads  $F_n$  were given to 4, 6, 8, 10 N. In the present test, the sliding time  $T$  for each test was set to 60 s. All tests were performed at room temperature without lubrication. The experimental scheme was designed with four different loads and four different sliding velocities as shown in Table 2.

**Table 1** Composition of 7050 aluminum alloy

Composition	Zn	Mg	Cu	Zr	Ti	Al
Contents (%)	5.7–6.7	1.9–2.6	2.0–2.6	0.08–0.15	≤0.06	Others

**Table 2** Ball-disc experimental parameters

No.	Load (N)	Sliding velocity (m/min)
1	4	90
2	6	90
3	8	90
4	10	90
5	4	120
6	6	120
7	8	120
8	10	120
9	4	150
10	6	150
11	8	150
12	10	150
13	4	180
14	6	180
15	8	180
16	10	180

### Details of surface morphology experiment

#### Theoretical analysis

In order to reveal the effect of average contact stress and sliding velocity on the friction coefficient, the average normal stress should be calculated first in the method of “Area Expansion”. During ball-disc friction experiment, the distribution of normal stress could be represented in Fig. 2.

In which,  $h$  is the depth of forming groove observed with the white light interferometer;  $w$  is the maximum width of ball-disc contact surface;  $l$  is half of ball-disc contact arc length. Then the average contact normal stress is obtained as Eq. 1 [12].

$$\sigma_{\text{ave}} = \frac{F_n}{w \cdot l} \quad (1)$$

In which,

$$w = \sqrt[3]{24 \cdot F_n \cdot R \cdot [(1 - \nu_1^2)/E_1 + (1 - \nu_2^2)/E_2]} \quad (2)$$

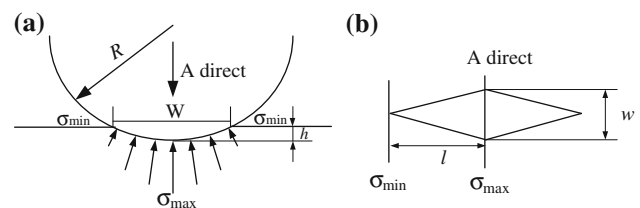


**Fig. 2** The analysis of average contact stress. **a** The distribution of normal stress. **b** Unfolded drawing of contact area

$$l = R \cdot \arccos\left(\frac{R-h}{R}\right) \tag{3}$$

where  $F_n$  is the load applying on the disc;  $R$  is the radius of cemented carbide ball;  $E_1$  and  $\nu_1$  are the elastic modulus and poisson ratio of cemented carbide ball, respectively;  $E_2$  and  $\nu_2$  are the elastic modulus and poisson ratio of Al7050-T7451, respectively. In the present study,  $R = 4.7625$  mm,  $E_1 = 611$  GPa,  $\nu_1 = 0.22$ ,  $E_2 = 71.7$  GPa,  $\nu_2 = 0.33$ .

Equipment and specimens

The white light interferometer (WLI) from Veeco Instruments with automated sample stage was used to observe the wear surface morphology of Al7050-T7451 after ball-disc experiment. WLI (shown in Fig. 3) is a powerful technique for non-contact measurement of surface topography at high vertical and moderate lateral resolution. Almost any surface can be measured, even quite dark ones. A number of data processing options are available, which makes it easy to analyze the surfaces quantitatively. The experimental specimen was the Al7050-T7451 disc after ball-disc friction experiment. Before observation, the specimen should be cleaned with alcohol.

Results and discussions

Sliding friction coefficient

The friction between carbide ball and Al7050-T7451 tends to reach stable state with the increase of sliding time, so the friction coefficient in the stable state is chosen as the results. The results and analysis of all tests are represented in Fig. 4.

As shown in Fig. 4, the friction coefficient decreases with the increasing of sliding velocity. With the growth of the load, the friction coefficient reduces evidently. At the same time, the effect of load on friction coefficient is larger than that of the sliding velocity. Otherwise, the influence of

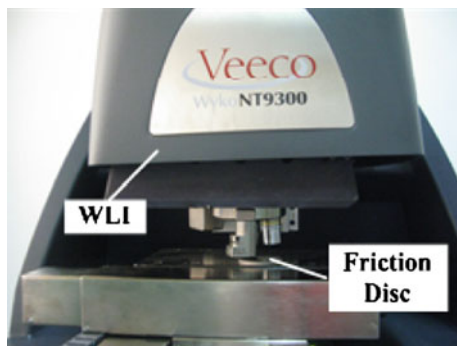


Fig. 3 White light interferometer

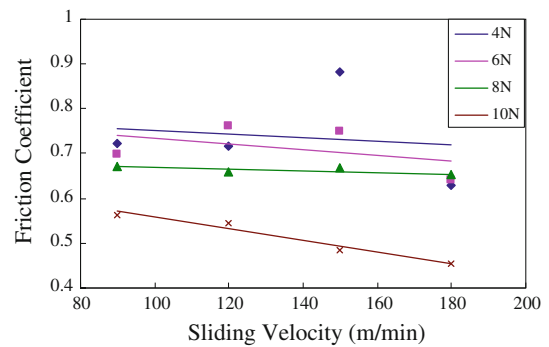


Fig. 4 The trend of friction coefficient with load and sliding velocity

load is not direct on the friction coefficient, and the value of average normal stress should be discussed in order to obtain the effect of average stress on the friction coefficient further.

Wear depth and average normal stress

The wear depth after ball-disc friction experiment is represented by the depth of forming groove. The NT9300 WLI made in American Wyko company is used to measure the depth and analyze the wear phenomenon. Figure 5 shows the measuring result of test No. 9. After measuring the depth of groove, calculate the corresponding average normal stress according to the Eqs (1–3). The testing results and corresponding analysis are listed in Fig. 6.

Equation fitting course

The exponential fit is used in engineering statistics widely. In the present article, the exponential equation also is used to fit the nonlinear relationship between the sliding friction coefficient and the average stress, the sliding velocity. Based on the experimental results which are listed in the Fig. 7, the initial equation form is defined as follow:

$$\mu = D \cdot v^i \cdot \sigma^j$$

where  $\mu$  is the sliding friction coefficient,  $v$  is sliding velocity, and  $\sigma$  is the average contact stress. Substituting the experimental data and fitting by means of statistical software Minitab, the fitting result is as follows:

$$\mu = 210.61 \cdot v^{-0.482} \cdot \sigma^{-0.857}$$

From the fitting results, it can be seen that the friction coefficient decreases with the growth of the sliding velocity and the average contact stress. Also the effect of the average contact stress is larger than that of the sliding velocity. According to the fitting formula, the friction coefficient can be calculated when machine the Al alloy with a certain velocity to make sure the determination of the friction coefficient in the finite element model.

**Fig. 5** The measuring result of WLI. **a** The profile of groove section. **b** The 3D graphic of groove

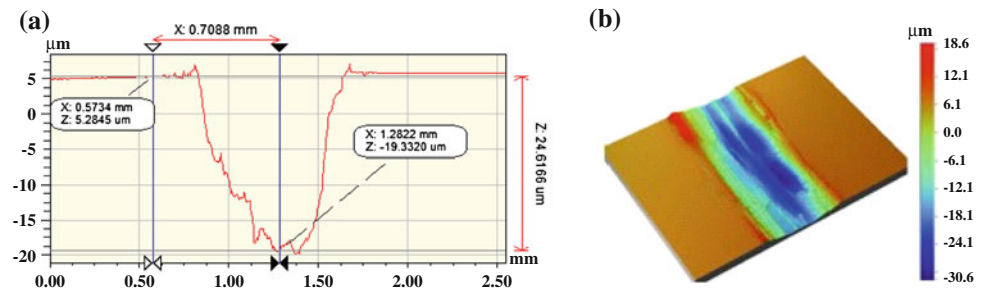


**Fig. 6** Results of the average normal stress. **a** Results with the same load. **b** Results with the same sliding velocity

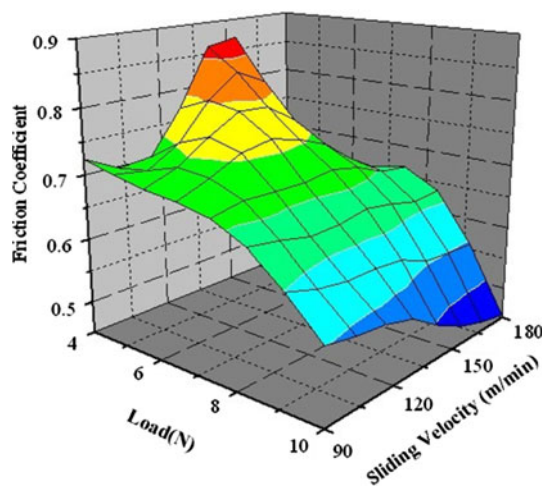
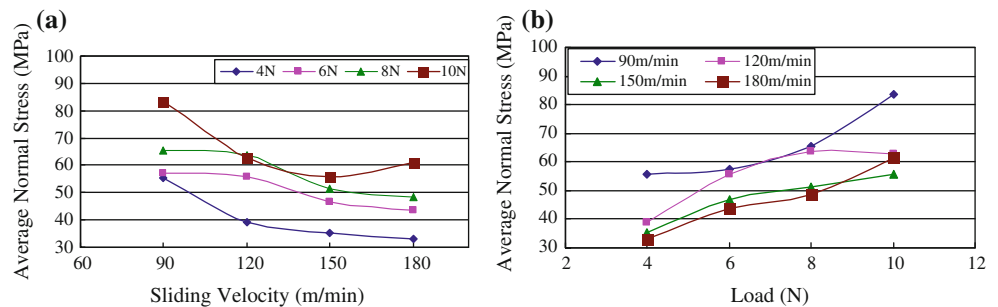


**Fig. 7** The experimental results of friction coefficient

## Conclusions

A series of tests have been performed to analyze the friction and wear behavior of Al7050-T7451 against YG8 cemented carbide. The following conclusions can be drawn:

- (1) The friction coefficient elevates first and then decreases with the increasing of load. The trend of the friction coefficient is different under smaller and larger load.
- (2) The average contact stress decreases with the increasing of sliding velocity, while increases with the increasing load.

- (3) The exponential fit is used to analyze the relationship between the sliding friction coefficient and the average contact stress, the sliding velocity. From the fitting result, the friction coefficient can be calculated to simulate the machining of Al alloy in the finite element model.

**Acknowledgements** This study is supported by Fundamental Technology Foundation of Chinese Education Department (No. A1420060196) and Specialized Research Fund for the Doctoral Program of Higher Education (No. 20070422033).

## References

1. Xiuli F, Xing A, Zhanqiang L et al (2007) China Mech Eng 18(2):220
2. Wan Y (2005) Study on the tool wear mechanism and tool life for high-speed milling aeronautic aluminium alloy [D]. Shandong University, Shandong
3. Bowden FP, Freitag EH (1958) Proc Roy Soc Lond A248:350
4. Bowden FP, Persson PA (1960) Proc Roy Soc Lond A260:433
5. Ogawa K (1997) Exp Mech 37(4):398
6. Rajagopalan S, Prakash V (1999) Exp Mech 39(4):295
7. Irfan MA, Prakash V (2000) Int J Solids Struct 37:2859
8. Okada M, Liou N-S, Prakash V, Miyoshi K (2000) Wear 249:672
9. Okada M, Liou NS, Prakash V (2001) Exp Mech 42(2):161
10. Liou NS, Okada M, Prakash V (2004) J Mech Phys Solids 52(9):2025
11. Yuan F, Liou NS, Prakash V (2009) Int J Plast 25:612
12. Carvill J. Mechanical Engineer's Data. 1.9 Contact stress, 51